5-2012

Conformational Motions Associated with Ligand Binding in Dihydrofolate Reductase from Bacillus stearothermophilus

Mayam Tobilola Alapa
Montclair State University

ABSTRACT

A fluorescently-labeled, conformationally-sensitive Bacillus stearothermophilus (*Bs*) dihydrofolate reductase (DHFR) (C73A/S131C$_{MDCC}$ DHFR) was developed and used to investigate kinetics and protein conformational motions associated with methotrexate (MTX) binding. This construct bears a covalently attached fluorophore, N-[2-(1-maleimidyl)ethyl]-7-(diethylamino)coumarin-3-carboxamide (MDCC) attached at a distal cysteine, introduced by mutagenesis. The probe is sensitive to the local molecular environment, reporting on changes in the protein structure associated with ligand binding. Intrinsic tryptophan fluorescence of the unlabeled Bs DHFR construct (C73A/S131C DHFR) also showed changes upon MTX association. Stopped-flow analysis of all data can be understood by invoking the presence of two native state DHFR conformers that bind to MTX at different rates (20.2 and 0.067 μM^{-1} s^{-1}), similar to previously published findings for Escherichia coli DHFR. Probe fluorescence of C73A/S131C$_{MDCC}$ DHFR predominantly reports on MTX binding to one of the conformers while intrinsic tryptophan fluorescence of C73A/S131C DHFR reports on binding to the other conformer. This study demonstrates the use of an extrinsic fluorophore attached to a distal region to investigate ligand binding interactions that are not experimentally accessible via intrinsic tryptophan fluorescence alone. The thermostability of C73A/S131C$_{MDCC}$ DHFR provides an important new tool with applications for investigating the temperature dependence of DHFR conformational changes associated with binding and catalysis.

MONTCLAIR STATE UNIVERSITY

CONFORMATIONAL MOTIONS ASSOCIATED WITH LIGAND BINDING IN DIHYDROFOLATE REDUCTASE FROM *BACILLUS STEAROTHERMOPHILUS*

by

Maryam T. Alapa

A Master's Thesis Submitted to the Faculty of
Montclair State University

In Partial Fulfillment of the Requirements
For the Degree of

MASTER OF SCIENCE

May 2012

College of Science and Mathematics

Department Chemistry and Biochemistry

Certified by:

[redacted]

Dr. Robert Prezant
Dean, College of Science and Mathematics

May 8, 2012
(Date)

Thesis Committee:

[redacted]

Dr. Nina M. Goodey
Thesis Sponsor

[redacted]

Dr. Johannes Schelvis
Committee Member

[redacted]

Dr. John Siekierka
Committee Member

[redacted]

Dr. Marc Kasner
Department Chairman

CONFORMATIONAL MOTIONS ASSOCIATED WITH LIGAND BINDING IN DIHYDROFOLATE REDUCTASE FROM *BACILLUS STEAROTHERMOPHILUS*

A THESIS

Submitted in partial fulfillment of the requirements

For the degree of Master of Science

by

MARYAM TOBILOLA ALAPA

Montclair State University

Montclair, NJ

2012

ACKNOWLEDGEMENTS

The greatest thanks belong to God for blessing me with success in my endeavors.

Special thanks to family and friends for their unending support, love and prayers; you all are the fuel that keeps me going. My family is my joy and I am glad I have a beautiful network of people that never stops encouraging and cheering me along. Special thanks to my best friend, for holding me together when I feel like cracking and for teaching me the important things in life. Never in a million years will I be able to show my mother how much I appreciate and love her. I dedicate this work to her; she is my rock and no one can ever take her place in my heart.

I offer sincere gratitude to my advisor, Dr. Nina Goodey, for her constant guidance, kindness and patience. Working with her has been a pleasure of mine and the growth I see in me is a result of her ability to cultivate a great and supportive environment where students not only learn but also mature in this field. She is always encouraging and is one of my greatest supporters. I could not have worked with a better advisor.

Thanks to the entire faculty at the department of Chemistry and Biochemistry. It is great to have a group of people who invest much time in one's success and are always ready to help when called upon. I will forever be grateful to you all.

I also say thanks to Montclair State University for offering me an admission, the last 6 years have been a great ride. Thanks to the Sokol Institute for funding my research and contributing to this success.

Thanks to the fellows and professors involved in the GK-12 program for their constant support and dedication. The program helped me transition from a shy student to a confident young lady. It was a great pleasure of mine to be in the program and I will forever treasure the memories.

Thank you to Alessandra, Tamara, Seema and Michael. It has been awesome to work with you all. Thank you for helping me through my thesis phase and prior to that.

CONTENTS:

LIST OF FIGURES:

1 Introduction

Dihydrofolate reductase (DHFR) is a ubiquitous enzyme that catalyzes the formation of tetrahydrofolate (THF) from dihydrofolate using NADPH as a cofactor. The need for THF in the synthesis of purines, thymidylate and a number of amino acids makes DHFR an important pharmaceutical target, especially for cancer and third world illnesses [1, 2]. Understanding its interaction with antifolates is useful for the rational design of new and improved inhibitors [3]. Enzymes exhibit two limiting binding mechanisms, first, induced fit, where ligand binding to free enzyme is followed by a conformational change that results in the preferred ligand-bound conformation, and second, conformational selection, where the ligand binds more rapidly to a specific enzyme conformation thus driving the conformational ensemble towards the faster binding conformer [4-6]. Such motions associated with ligand binding can be critical for efficient inhibition as well as discrimination between ligands [5, 7]. Methotrexate (MTX) and trimethoprim (TMP) are competitive DHFR inhibitors; they have been demonstrated to influence DHFR dynamics distal to the active site with the role of the abrogation of dynamics in inhibiting catalysis the subject of some discussion [3, 8].

The conformational motions of *E. coli* DHFR have been explored using many different methods and it has become a paradigm for understanding the relationship between structure, dynamics and catalysis [3, 9-12]. Long range coupling that occurs between the active site and distal regions has been previously observed in both experimental and theoretical studies [3, 13-15]. Two-dimensional NMR studies revealed that the apo enzyme exists in at least two equilibrium conformations that have different binding affinities for the substrate and cofactor [16-20]. X-ray crystallography studies on

E. coli DHFR have revealed multiple conformations of the enzyme for different ligand bound states including the closed, occluded, and open conformations; the largest structural differences observed in the X-ray structures are in the Met20 loop that closes upon the active site [11, 21]. In an ensemble and single molecule kinetics study, Rajagopalan and coworkers [22] attached an extrinsic fluorophore to the active site Met20 loop and found that the two native state conformers of *E. coli* DHFR are capable of binding MTX with different association rates [22].

DHFR isolated from *Bacillus stearothermophilus* (*Bs*) is a thermostable monomer with a mass of 18.7 kDa [23]. An X-ray structure published by Kim and coauthors showed the highly conserved globular α/β DHFR structure consisting of eight β-sheets and four α-helices and revealed *Bs* DHFR as the first monomeric DHFR from a thermophilic organism (Figure 1) [23]. *Bs* DHFR has catalytic properties that lie between those of the *E. coli* and *T. maritima* homologs [23-25].

The themostability of *Bs* DHFR combined with its typical catalytic properties make it an excellent DHFR model for studies of conformational motions. For this study, the distal residue Ser131 was replaced by a Cys and labeled with an environmentally sensitive fluorescent dye *N*-[2-(1-maleimidyl)ethyl]-7-(diethylamino)coumarin-3-carboxamide (MDCC) to create a labeled construct, C73A/S131C$_{MDCC}$ DHFR. This construct was used to investigate MTX binding and associated conformational changes of *Bs* DHFR. In our study, the probe on *Bs* DHFR is distal to the binding site and does not strongly respond to the presence or absence of MTX but rather to conformational changes propagating to distal regions. Here we report a new conformationally sensitive *Bs* DHFR construct with a fluorophore in a distal position. We demonstrate the usefulness of this

new construct in studies of the binding mechanism and associated conformational motions upon ligand binding.

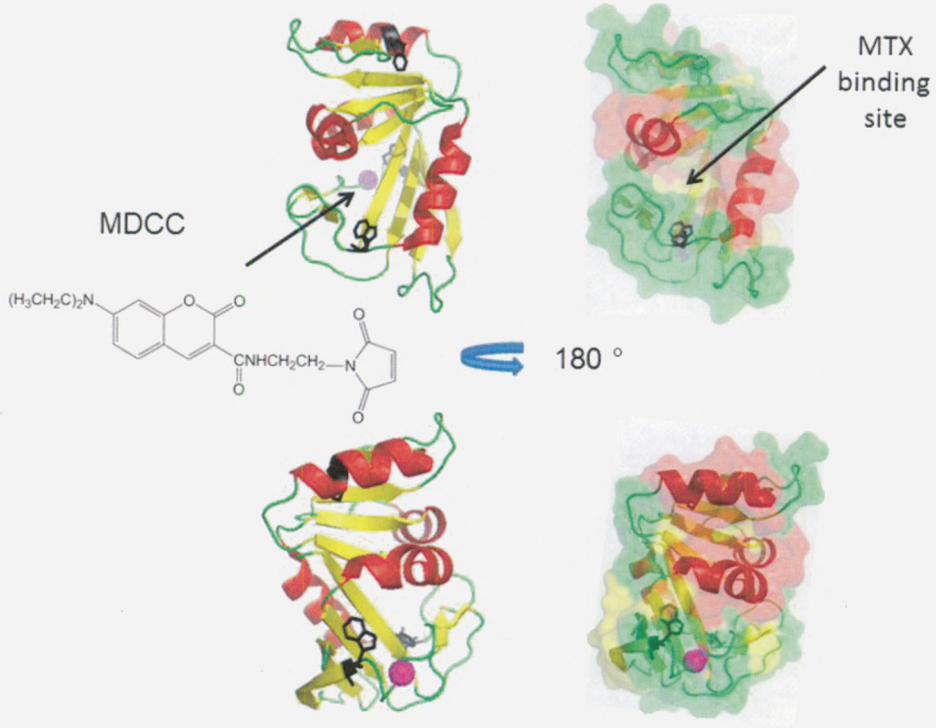

Figure 1. A cartoon (left) and surface (right) representation of the structure of *Bs* DHFR (PDB ID: 1ZDR). Residue 131, the site of labeling, is shown as a magenta sphere. The MTX binding site is labeled in the surface representation.

2 Material and methods

2.1 Construction of mutant genes

The pet21a (+) vector containing the *Bs* DHFR gene (kindly donated by Judith P. Klinman) was subjected to QuickChange mutagenesis (Stratagene) to introduce the C73A and S131C replacements using the following primers: C73A – 5'-CGC CCG GAA GGC GCC CTT GTG CTT CAT TCG-3' (forward) and 5'-CGA ATG AAG CAC AAG GGC GCC TTC CGG GCG-3' (reverse); and S131C - 5'-GAT ACG TTT TAT CCG CCC ATT TGT GAC GAT GAA TGG-3' (forward) and 5'-CCA TTC ATC GTC ACA AAT GGG CGG ATA AAA CGT ATC-3' (reverse). The desired sequences were confirmed by complete sequencing of the genes.

2.2 Protein expression and purification

The unlabeled *Bs DHFR* construct (C73A/S131C DHFR) was expressed in *E. coli* BL21 cells grown in LB broth containing 100 μg/mL ampicillin at 37 °C. When OD_{600} reached 0.6, expression was induced using 1 mM isopropyl-β-D-thiogalactopyranoside (IPTG) and the cells were grown for 12-16 h. Cells were centrifuged, washed in 0.9% NaCl, and centrifuged again. The cells were suspended in 40 mM *N*-2-hydroxyethylpiperazine-*N*'-2-ethanelsulfonic acid (HEPES) buffer at pH 6.8, then lysed by sonication. The supernatant was incubated at 55 °C for 20 min and centrifuged to remove precipitated proteins. The supernatant was loaded onto an SP-sepharose C-25 column and eluted with 0.2 M NaCl in 40 mM HEPES (pH 6.8). The DHFR fractions were collected, exchanged into 40 mM HEPES (pH 6.8), concentrated, and stored at -80 °C. The protein was determined to be >95 % pure by SDS-PAGE electrophoresis (Figure 3).

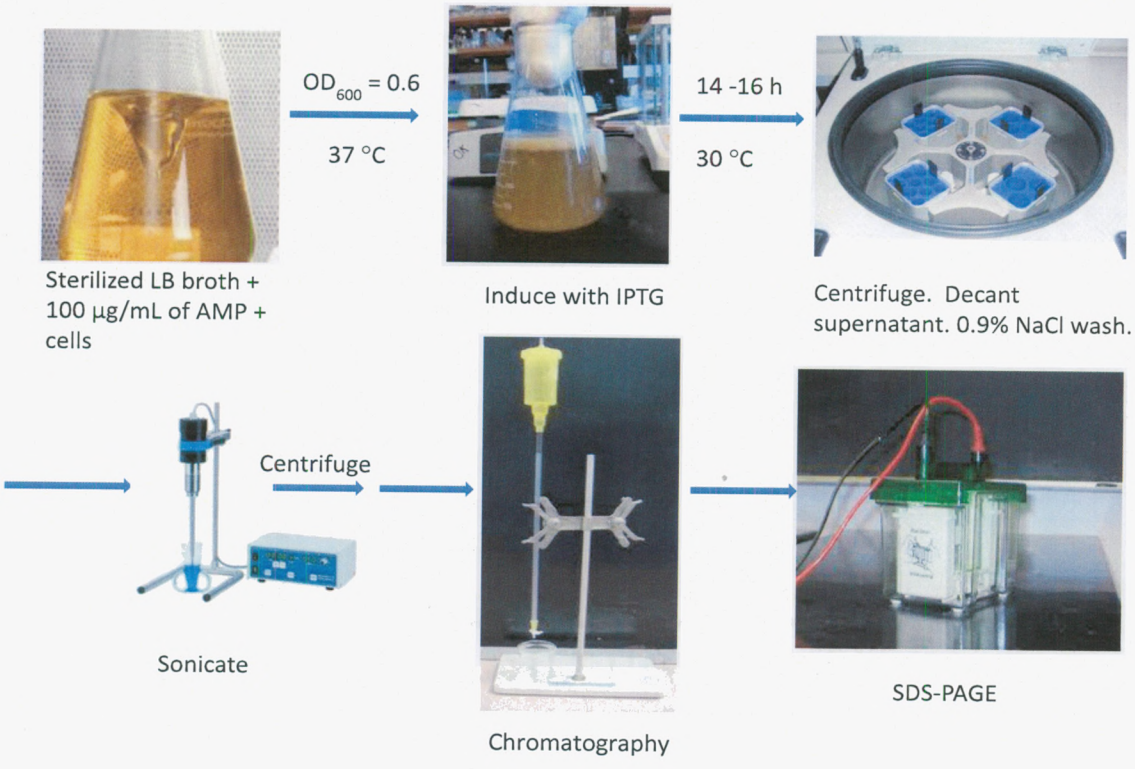

Figure 2. A schematic view of the purification process.

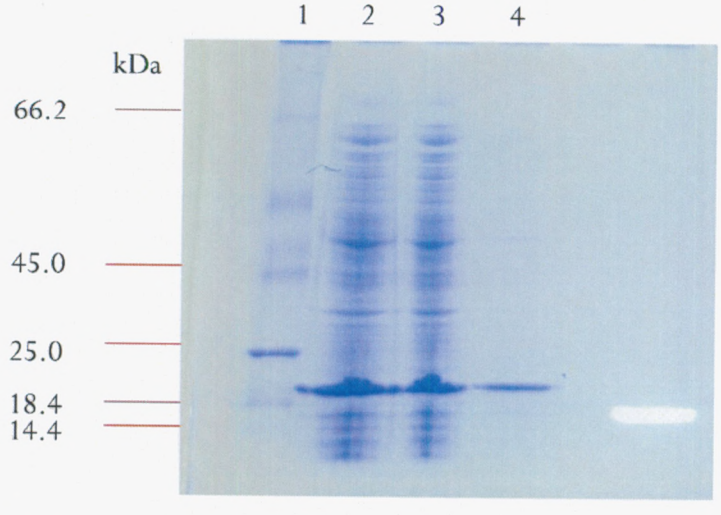

Figure 3. SDS-PAGE gel of protein purification. Lane 1: protein marker in kDa; Lane 2: supernatant from the expressed cell extract; Lane 3: pool of fractions from column wash; Lane 4: pure C73A/S131C DHFR ~18.4 KDa.

2.3 Preparation of C73A/S131C$_{MDCC}$ DHFR

The labeling was initiated by adding a 3-fold molar excess of 2.26 mM stock solution of MDCC fluorophore (MW 383.4 g/mol) dissolved in dimethyl sulfoxide to a solution of purified C73A/S131C DHFR to obtain final dye and enzyme concentrations of 93.3 and 32.1 μM, respectively. The mixture was covered with aluminum foil to protect the sample from light and incubated at room temperature for 2 h. The sample was dialyzed twice for 4 h at 4 °C into 40 mM HEPES at pH 7.2 to remove free dye and to exchange buffer. Labeling efficiency was found to be ~97.4 % from absorbance measurements at 280 and 419 nm using a Thermo Scientific NanoDrop 2000c UV-Vis spectrophotometer.

2.4 Measurement of equilibrium dissociation constants (K_D)

Equilibrium dissociation constants were measured using fluorescence quenching as previously described [26] by following the quenching of the intrinsic Trp fluorescence of C73A/S131C DHFR (290 nm excitation and 340 nm emission) and MDCC fluorescence of C73A/S131C$_{MDCC}$ DHFR (419 nm excitation and 466 nm emission) as a function of added ligand concentration using a FluoroMax4 spectrofluorometer by Horiba. The binding curves were corrected for dilution by buffer and fitted using the Morrison equation [27] to obtain K_D values.

2.5 MTX binding kinetics

MTX (0.4 - 200 μM for unlabeled C73A/S131C DHFR and 0.4 - 200 μM for C73A/S131C$_{MDCC}$ DHFR) was mixed with 2 μM enzyme in MTEN buffer (50 mM 2-(*N*-morpholino) ethanesulfonic acid, 25 mM tris(hydroxymethyl)-aminomethane, 25 mM

ethanolamine, and 100 mM NaCl) at pH 7 at rt in an Applied Photophysics SX20 stopped-flow instrument. The resulting changes in fluorescence emission intensity for C73A/S131C DHFR (excitation at 290 nm, emission with a 320 nm cutoff filter) and C73A/S131C$_{MDCC}$ (excitation at 419 nm, emission with a 450 nm cutoff filter) were recorded. A minimum of five individual traces were averaged to obtain an average trace for each ligand concentration.

To measure the dissociation rate of the DHFR-MTX complex, 2 μM enzyme was incubated with 4 μM MTX in MTEN buffer at pH 7.0. The enzyme-ligand solution was then mixed in a stopped-flow apparatus with either 350 μM or 700 μM TMP to displace MTX. The dissociation event was monitored by following the fluorescence emission changes (ex./em. 290 nm/320 nm cutoff filter and 419 nm/450 nm cutoff filter for C73A/S131C DHFR and C73A/S131C$_{MDCC}$ DHFR, respectively). Stopped-flow fluorescence emission data were fitted using DYNAFIT [28].

2.6 Temperature study

2 μM each enzyme construct was mixed with Mtx (2.5 – 20 μM) in the stopped flow instrument. The concentration of enzyme and ligand was kept constant while the temperature was slowly increased from 10 – 45 °C using a water bath PolyScience. The changes in emission intensity were recorded for the C73A/S131C DHFR construct (ex. 290 nm and 320 nm cutoff filter) and C73A/S131C$_{MDCC}$ DHFR construct (ex. 419 nm and 450 nm cutoff filter). Four to five data traces were averaged at each temperature. Thermodynamic values were obtained by using the Arrhenius[29] equation (equation 1) and the Eyring equation (equation 2) [30].

$$\ln(k) = -\frac{Ea}{R}\left(\frac{1}{T}\right) + \ln A \qquad 1$$

$$\ln\left(\frac{k}{T}\right) = -\frac{\Delta H^{\circ}}{R}\left(\frac{1}{T}\right) + \ln\left(\frac{kB}{h}\right) + \frac{\Delta S^{\circ}}{R} \qquad 2$$

3 Results and Discussion

3.1 Effect of MTX binding on Trp fluorescence of C73A/S131C DHFR

Intrinsic tryptophan fluorescence combined with stopped-flow instrumentation is an established method for studying the kinetics of protein-ligand binding that, for some systems, allows detection of some associated conformational motions. For an example, see work presented by Cameron and coworkers [31]. There are three tryptophans in *Bs* DHFR (Trp22, Trp85 and Trp135). While Trp85 and Tpr135 are distal to the MTX binding site, Trp22 is located on a loop that aligns with the active site Met20 loop from *E. coli* DHFR (residues 9-23). The Met20 loop of *E. coli* DHFR has been shown to adopt multiple conformations (open, closed, occluded) and play a role in ligand binding and catalysis [3, 9, 11]. Thus Trp22 fluorescence likely responds to the presence or absence of MTX in the binding site, perhaps explaining at least in part the observed tryptophan signal upon MTX binding.

To study the binding kinetics between *Bs* DHFR and MTX, 2 μM C73A/S131C DHFR was rapidly mixed with 1.25 – 200 μM MTX in a stopped flow instrument and the time course of tryptophan fluorescence emission intensity (ex. 290 nm, em. 320 nm cutoff filter) was recorded (Figure 4). For all ligand concentrations, a trace with a large ligand concentration dependent decrease was observed. The fluorescence emission intensity versus time traces were satisfactorily fitted by a single exponential equation at low ligand concentrations (1.25 – 20 μM). The MTX concentration dependence of the

rate constant for the fast phase (single exponential fit) was linear with a slope of 23 $\mu M^{-1}s^{-1}$ and an intercept of -0.0655 ± 0.0388 (no figure). For higher ligand concentrations (50 – 100 μM), a large ligand concentration dependent decrease followed by a second, small, ligand-concentration-independent decrease and a two-step mechanism was required to fit the data (Figure 4). The ligand-concentration-dependent signal was attributed to binding of MTX to enzyme and the small, ligand-concentration-independent signal to a conformational motion following ligand binding. The two-step mechanism shown in Figure 4 was used to fit traces with different substrate concentrations from parallel runs in a "global fit". The second, MTX concentration independent phase allowed us to determine the rate of the E.MTX →E'.MTX' (k_2) conformational change using DYNAFIT (Figure 4B) [28]. The first phase corresponds to the E to MTX association, k_1, and the second phase (6.25% of the total signal) is attributed the conformational change of E.MTX to E'.MTX

governed by k_2 and k_{-2}. The rate constant that best fits this second phase is approximately 10 $\mu M^{-1}s^{-1}$ (k_2); k_{-2} was unresolved. Due to small signal amplitude, there is some uncertainty associated with the optimal value for k_2.

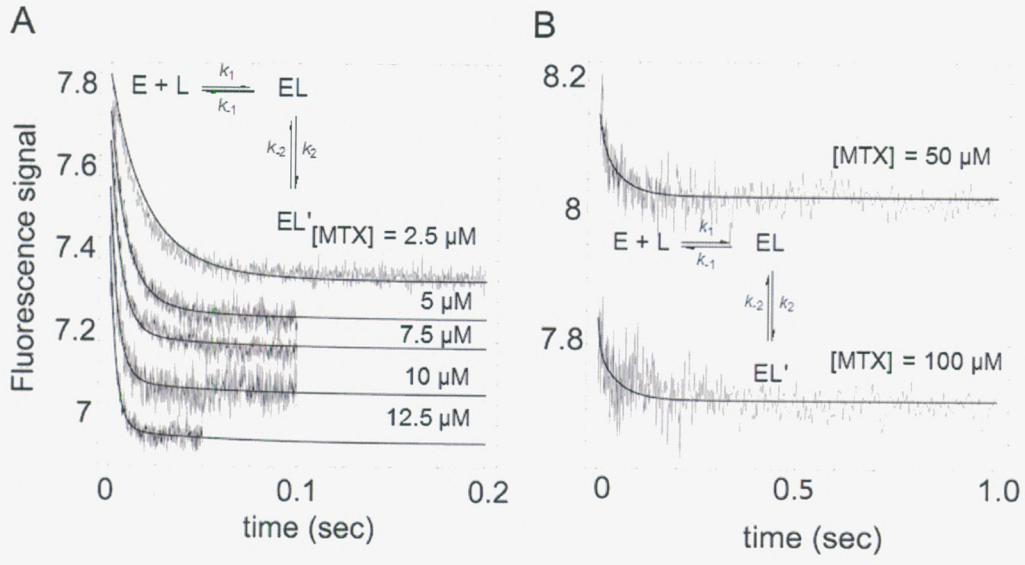

Figure 4. The time dependence of tryptophan fluorescence emission intensity (ex. 290 nm, em. 320 nm cutoff filter) during MTX association. The smooth lines show the best fit obtained by nonlinear regression fitting data to the model shown using Dynafit. (A). In the stopped-flow instrument, equal volumes of 2 μM C73A/S131C DHFR and 5 – 25 μM MTX were mixed and tryptophan emission intensity was monitored. The traces fit best to an association rate (k_1) of 20.2 $\mu M^{-1}s^{-1} \pm 0.21$. (B). Tryptophan fluorescence traces at a higher ligand concentrations. Equal volumes of 2 μM C73A/S131C DHFR and 50 μM or 100 μM MTX were mixed and the signal was monitored. At higher ligand concentrations, the concentration independent step with small amplitude (E.MTX to E'.MTX) can be clearly observed due to the faster binding rate of the ligand-concentration-dependent step; the best value for k_2 was determined to be 9.9 $\mu M^{-1}s^{-1} \pm 0.75$.

The dissociation rate for the E.MTX complex was determined by stopped-flow instrumentation using TMP to displace MTX from the E.MTX complex. An increase in tryptophan fluorescence (600 s trace) was observed upon mixing 350 μM TMP with 2 μM C73A/S131C DHFR pre-incubated with 4 μM MTX. The trace fits satisfactorily to a single exponential equation (no figure) with an MTX dissociation rate of 0.01 s^{-1} that is independent of TMP concentration (similar results were obtained with 700 μM TMP). A similar value was previously observed for MTX dissociation from *E. coli* DHFR [22].

3.2 Effect of MTX binding on MDCC fluorescence of C73A/S131C$_{MDCC}$ DHFR

Cys73, the only naturally occurring cysteine residue in *Bs* DHFR, was replaced by an alanine via mutagenesis (C73A) to prevent MDCC attachment at multiple sites. Distal Ser131, located between the loop that connects β-sheets 8 and 9, was replaced by Cys to introduce a reactive handle to *Bs* DHFR and the environmentally sensitive fluorophore MDCC was covalently attached to this position (Figure 1). Position 131 is distal to the MTX binding site: the distance between the serine side chain oxygen and the βC of Asp27, which is involved in MTX binding, is 23.9 Å (PDB ID: 1ZDR). These replacements (C73A/S131C) did not significantly influence the turnover number (unpublished data). The K_D values of MTX for wildtype *Bs* DHFR and C73A/S131C DHFR were found to be 17 ± 3 nM and 42.7 ± 10 nM, respectively. We determined a K_D value of 39 ± 0.92 nM for C73A/S131C$_{MDCC}$ DHFR, indicating that introduction of the mutations or fluorophore attachment did not significantly interfere with MTX binding and that C73A/S131C$_{MDCC}$ DHFR is a good model for wildtype *Bs* DHFR.

When 2 μM C73A/S131C$_{MDCC}$ DHFR was mixed with 0.4 - 200 μM MTX, a decrease of ~26.0 % in fluorescence emission intensity (ex. 419 nm, em. 450 nm cutoff filter) was observed. When the traces were fitted to a single exponential equation, the ligand concentration dependence of the observed rate constant was found to be linear with a slope of 0.07 $\mu M^{-1}s^{-1}$ and a nonzero intercept (Figure 5A). This signal was attributed to binding of a second conformer of *Bs* DHFR (E') to MTX to form E'.MTX. Probe fluorescence is predominantly (90.5 % of the signal) influenced by binding of MTX to DHFR conformer E'. A fast, decreasing burst with a small amplitude (~9.5% of total signal amplitude) is also observed upon mixing of the enzyme and MTX (inset in

Figure 5A) and can be fitted with a second order rate constant of 24 $\mu M^{-1}s^{-1} \pm 1.9$. This small signal is attributed to binding of E to MTX. Consequently, the traces were fitted to a mechanism (shown in Figure 5A) that included binding of E to MTX and E' to MTX. We tried to isolate tryptophan signal of the C73A/S131C$_{MDCC}$ DHFR construct to confirm that the event occurring at a rate of 24 $\mu M^{-1}s^{-1}$ indeed corresponds to binding of MTX to E. Unfortunately, for C73A/S131C$_{MDCC}$ DHFR, similar results were obtained at both detection wavelengths (290 nm excitation with 320 nm cut off filter and 419 nm excitation with 450 nm cutoff filter) due to spectral overlap and the high quantum yield of the probe relative to tryptophan. Nevertheless, the small, initial burst at 24 $\mu M^{-1}s^{-1}$ observed in MDCC fluorescence likely corresponds to the binding event observed for C73A/S131C DHFR by Trp fluorescence.

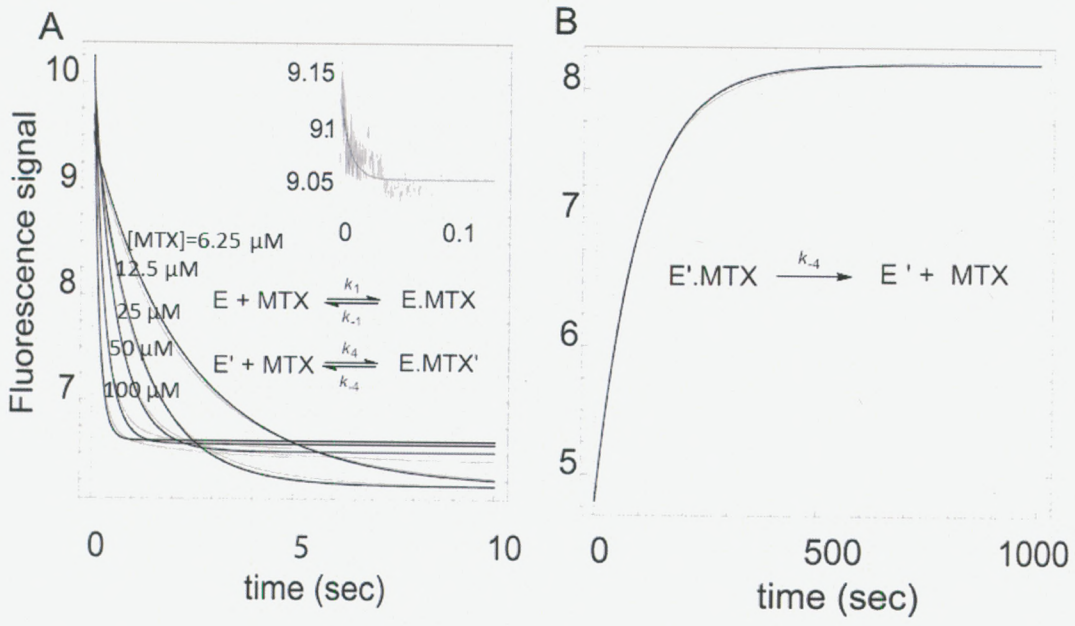

Figure 5. Stopped-flow experiments on MTX and C73A/S131C$_{MDCC}$ DHFR association and dissociation monitoring probe fluorescence. (A). Equal volumes of 2 μM C73A/S131C$_{MDCC}$ DHFR and 13 – 200 μM MTX were mixed and the probe fluorescence

(ex. 419 nm and em. 450 nm cutoff filter) was monitored. The traces were fitted to the mechanism shown; the solid lines represent the fit while the thin lines show the data. The best value for k_1 is 23.99 $\mu M^{-1}s^{-1} \pm 1.9$. The inset shows the fast burst observed at short times (first 0.1 s). This was also fitted to the same k_1 value and represents the predominant signal from the tryptophan experiment. (B) The dissociation of MTX from the enzyme-ligand complex. The experiment was carried out by pre-incubating 2 μM C73A/S131C$_{MDCC}$ DHFR with 4 μM MTX. The mixture was then inserted into the stopped flow instrument and rapidly mixed with 350 μM TMP replacing MTX from the enzyme's binding site and resulting in an increase in the fluorescence signal. The k_{-4} value obtained by fitting this data to a simple dissociation mechanism (see above) is 0.01 $s^{-1} \pm 0.0004$.

To measure the rate of MTX dissociation from E'.MTX, 2 μM C73A/S131C$_{MDCC}$ DHFR was incubated with 4 μM MTX and then mixed with 350 μM TMP in the stopped-flow instrument (Figure 5B). An increase in the fluorescence emission intensity was observed due to the replacement of MTX by TMP in the binding site. The observed signal was fitted to a single-exponential equation and yielded a dissociation rate (k_{-4}) of 0.01 $s^{-1} \pm 0.0004$; a similar rate was measured for dissociation of MTX from C73A/S131C DHFR by measuring changes in fluorescence (k_{-1}). A similar value of 0.0155 s^{-1} was previously reported for the dissociation of MTX from *E.coli* DHFR [22]. Figure 6 shows a model that is consistent with all data from the kinetic experiments, both using probe fluorescence and intrinsic tryptophan signal; the rates that are consistent with our data are shown in Table 1. A similar model has previously been published for *E. coli* DHFR [17, 18, 22].

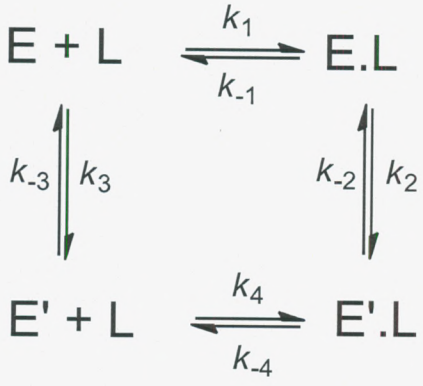

Figure 6. The minimal model for MTX binding to *Bs* DHFR. E and E' represent different conformational states of *Bs* DHFR. The rate constants are first order rate constants in units of s^{-1} except for the ligand binding steps which are second order rate constants ($\mu M^{-1} s^{-1}$). The induced fit pathway follows steps with k_1 and k_2. Binding of MTX to E forms the initial complex E.MTX which is not stable because the conformation is not optimized and can convert to E'.MTX. The conformational selection pathway follows steps with k_3 and k_4 or with k_{-3} and k_1. The step with k_3 and k_{-3} describes the conformational equilibrium between the two different *Bs* DHFR conformations (E and E'). The step with k_4 shows the binding of MTX to conformer E'.

Table 1. The table shows a summary of rate constants that best fit the data. The observed rate increases with higher ligand concentration for k_1 and k_4.

Rate Constant	Rate	Error	Experiment
k_1 ($\mu M^{-1} s^{-1}$)	20.2	± 0.21	Trp fluorescence (low ligand concentrations)
	23.99	±1.9	Probe fluorescence
k_{-1} (s^{-1})	0.01	± .00002	Competition experiment, trp fluorescence
k_2 (s^{-1})	9.9	± 0.75	Trp fluorescence (high ligand concentrations)
k_{-2} (s^{-1})	NA		NA
k_4 ($\mu M^{-1}/s^{-1}$)	0.067	± 0.0001	Probe fluorescence
k_{-4} (s^{-1})	0.01	±0.00041	Competition experiment, probe fluoresence

*k_2 from Trp fluorescence (low ligand concentration) is 10.1 s^{-1} ± 0.38.

3.3 Temperature study

Bs DHFR is a thermostable enzyme, which allows scientists to study the enzyme at a wide range of temperature and learn more about the binding kinetics. *Bs* DHFR has a higher melting temperature, which renders it more stable than *E.coli* DHFR. Previous study on *Bs* DHFR in D_2O shows that the enzyme is stable at a temperature of 10 °C for 4 h and unfolding occurs at a temperature of 65 °C after 11 min [32]. Some of the

structural elements in *Bs* DHFR are longer when compared to its homologues and the higher number of amino acids in the secondary structure may contribute to its overall stability at higher temperatures [23].

In many cases, reaction and binding rates increase with increasing temperatures. Both the Arrhenius (equation 1) and the Eyring (equation 2) equations can be used to describe the temperature dependence of reaction and/or binding rates. Analysis of the temperature dependence can provide insights into the energy barrier between the unbound species and the complex or the energy barrier between the two conformations of the enzyme. Application of the Eyring equation can be used to calculate the entropic and enthalpic contributions to the energetic barrier to an association event or a conformational change. The enthalpic contribution to the energetic barrier, $\Delta H^{\neq}$, represents the difference between the enthalpy of the transition state and the sum of the enthalpies of the reactants in the ground state. It is often called activation enthalpy. The $\Delta S^{\neq}$ gives information about the degree of order in the transition state. Large, negative values of $\Delta S^{\neq}$ suggest that the transition state complex is more ordered or rigid than the reactants (E and ligand) in the ground state. A less negative value for $\Delta S^{\neq}$ would indicate that the transition state is disordered compared to the ground state.

The linear form of the Eyring equation is shown in equation 2 in the form $y = -mx + b$. A plot of $\ln(k/T)$ versus $1/T$ produces a straight line where m is $\Delta H^{\neq}$ and the y-intercept represents $\Delta S^{\neq}$.

When the temperature dependence of binding rate constant k_1 from Table 2 was investigated and that data was plotted where $y = \ln (k/T)$ and $x = 1/T$ (1/K), a linear relationship between the rate and temperature observed for temperatures ranging from 10

– 45 °C (Graph 1-3). The linearity of the relationship suggests that the enzyme molecules are not unfolding at the temperature range of study. The lower temperature limit of 10 °C was used to avoid freezing the protein and keeping it from undergoing cold denaturation. The final ligand and enzyme concentration were kept constant, 2.5 μM and 2 μM, respectively, while the temperature was changed.

Table 2
The summary of thermodynamic values derived using the Arrhenius equation and Eyring equations. The final concentrations are 1 μM for the enzyme and 2.5 μM for the ligand.

Signal	Step	E_a	$\Delta H^{\neq}$	$\Delta S^{\neq}$	$\Delta G^{\neq}_{(298\ K)}$
		(Kcal/mol)	(Kcal/mol)	(J/mol-K)	(Kcal/mol)
Trp	Binding	-6.1	-5.5	-124.6	3.36
	Conformational change	-6.5	-12.3	-64.2	-7.74
Probe	Binding	-14	-13.3	-78	-7.71

Both the binding event (E + MTX to E.MTX) and the conformational change (E.MTX to E.MTX') can be investigated by measuring changes in the Trp fluorescence signal after the enzyme and ligand are mixed as described above in section 2.6. When the rate constants are plotted against the inverse temperature and fitted to a linear equation, the $\Delta H^{\neq}$ and $\Delta S^{\neq}$ can be obtained for each phase of the signal (binding k_1 and conformational change k_2) (table 2). The $\Delta H^{\neq}$ value is a larger negative value (-12.3 kcal/mol) for the conformational change compared to the value for the binding event (-5.5 kcal/mol). This observation suggests that the enthalpic contribution to the reaction barrier is greater for the enzyme-ligand complex conformational change than for the binding of Mtx to the enzyme. The activation entropy $\Delta S^{\neq}$ values are negative for the binding steps. This is not surprising because degrees of freedom are lost when two molecules come together and form a complex. The activation entropy for the conformational change is also negative indicating that there is a loss of degrees of

freedom in the transition state compared to the starting conformation. The conformational change has a large, negative entropic contribution to the reaction barrier.

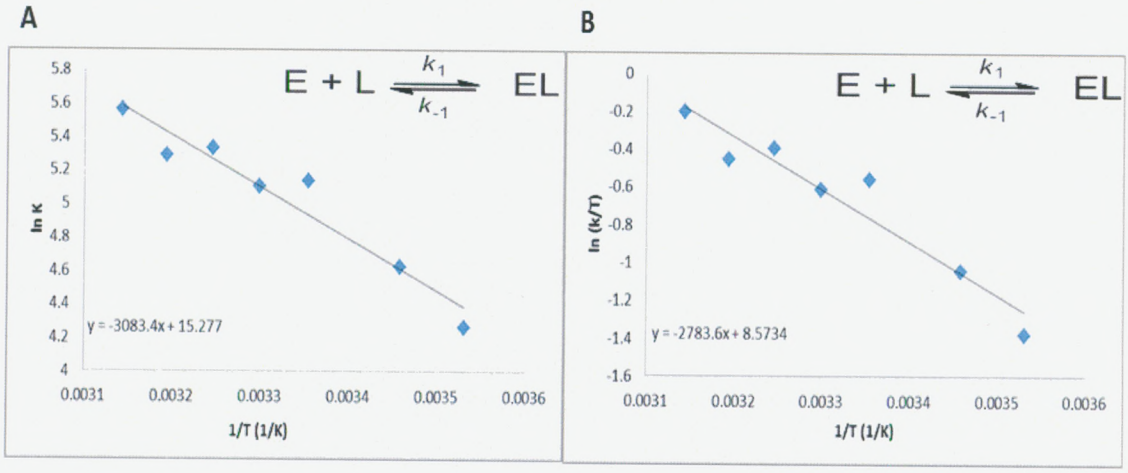

Graph 1. Plots of natural log of k_{obs} and ln (k_{obs}/T) *vs*. inverse temperature of the binding step (Figure 4A). (A) The temperature effect of the Mtx binding to the C73A/S131C construct. The plot is linear; the rate increases with temperature, which ranges from 10 - 45°C. The slope, -3083.4, of the graph was used to determine the energy of activation. (B) Plot of ln (k/T) *vs*. 1/T, where the slope is -2783.6 and y-intercept is 8.5734, were used to determine the enthalpy and entropy change of the transition state. The final concentration of enzyme is 1 μM and that of Mtx is 2.5 μM (ex. 290 nm and 320 nm cutoff filter).

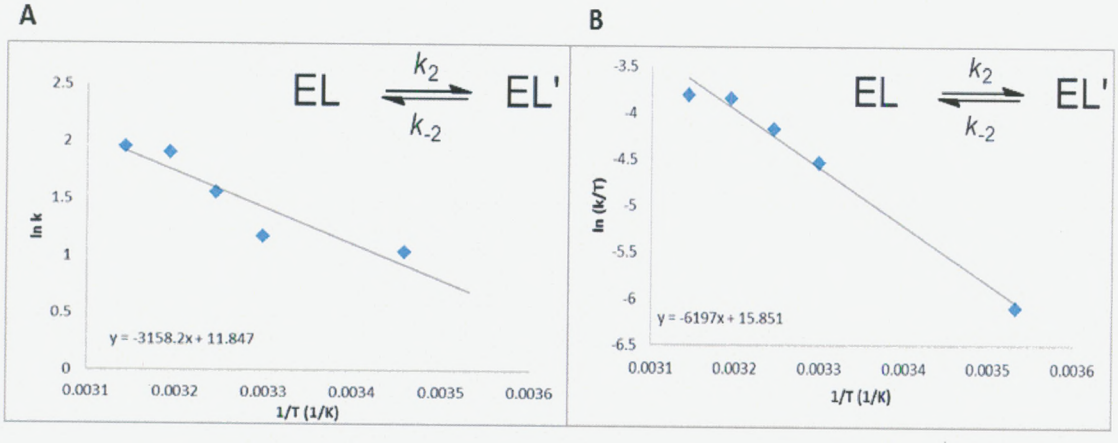

Graph 2. Plot of ln (k_{obs}/T) *vs*. inverse temperature of the conformational change (Figure 4B). (A) The temperature effect on the conformational change of the EL to EL' in the C73A/S131C DHFR construct. The slope, -3125.2, was used to determine the energy of activation using the Arrhenius equation. (B) The slope, -6197, and y-intercept, 15.851, were used to determine the transition state enthalpy and entropy change of the

conformational modification of the enzyme-ligand complex. The rate of the conformational change increases with temperature.

There is a linear relationship between rate (k_4) and temperature when Mtx binding to the second conformer, E'. Thermodynamic parameters can also be acquired for the binding of E' to Mtx (Graph 3), an event that is detected by measuring changes in the MDCC probe signal. Here, the energy of activation and change in enthalpy on the energy barrier are significantly higher than those observed by detecting the Trp signal. A more negative value for the energy of activation is observed in the binding step E' + L to EL' compared to the Trp signal (E + Mtx to EMtx), the values are -14.0 kcal/mol and -6.1 kcal/mol, respectively. The overall energy of activation is favorable at room temperature due to the decrease in enthalpy. In the binding step, the Gibbs free energy change, $\Delta G^{\neq}$, in the lower binding conformer, E', is more favorable (-7.71 Kcal/mol) than the energy of the faster binding conformer E, which is 3.36 Kcal/mol.

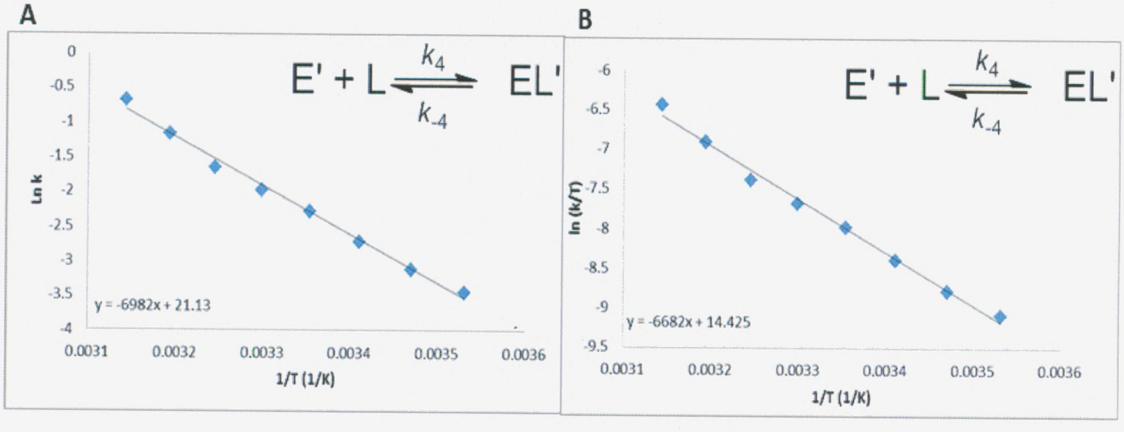

Graph 3. Plots of natural log of k_{obs} and ln (k_{obs}/T) *vs.* inverse temperature of the binding step in C73A/S131C$_{MDCC}$ DHFR construct (Figure 5A). (A) The slope, -6982, was used to determine the energy of activation when E' binds to Mtx, as observed by the probe (MDCC). (B) The slope, -6682, and y-intercept, 14.425, were used to determine the enthalpy and entropy change of the transition state. The final concentration of enzyme is 1 μM and that of Mtx is 2.5 μM (ex. 419 nm and 450 nm cutoff filter). The temperature

range is 10 – 45 °C and the linear plot shows that denaturation does not occur at the temperature range.

4 Summary

The kinetic data are consistent with a mechanism where unbound *Bs* DHFR exists in two conformations, E and E', and MTX can bind to both states (Figure 6). Binding of E' to MTX to form E'.MTX occurs at a rate of 0.067 $\mu M^{-1}s^{-1} \pm 0.0001$. The rate constant for MTX association with E' is approximately 10 times faster for *E. coli* DHFR compared to *Bs* DHFR and this difference may reflect the rigidity of the thermostable *Bs* DHFR compared to the *E. coli* homolog [22]. Binding of MTX to E also results in a small amplitude burst in MDCC fluorescence for the C73A/S131C$_{MDCC}$ DHFR construct (Table 1). Tryptophan fluorescence of the unlabeled C73A/S131C DHFR reports on the binding of E to MTX and gives a k_1 rate of 20.2 $\mu M^{-1}s^{-1} \pm 0.21$ in a global fit. Tryptophan fluorescence of the C73A/S131C DHFR construct at high MTX concentrations revealed that binding of E to MTX is followed by a conformational change of E.MTX to E'.MTX at a rate of 10 $\mu M^{-1}s^{-1} \pm 0.75$. Tryptophan fluorescence does not provide any information on binding of E' to MTX.

MDCC displays only small response to the presence or absence of MTX in the binding pocket (binding of MTX to the conformer E, ~9.5% of signal amplitude (inset in Figure 5A)) but rather senses conformational changes that influence the environment on residue 131. The relatively weak and slow binding of E' to MTX is consistent with a conformational motion that is associated with binding that causes a change in probe environment. The origin of the change (specific conformational event) in the probe environment associated with MTX binding is currently unknown. Attaching probes to

different distal regions of DHFR will reveal whether the motion of E' influences the environments of other regions. The relatively slow rates of binding allows the study of *Bs* DHFR ligand binding interactions by stopped flow techniques even at higher temperatures. The C73A/S131C$_{MDCC}$ DHFR construct provides a valuable tool to understand the impact of dynamics on protein function of conformer E' as the stability of the enzyme at higher temperatures allows a wide temperature range to be accessed. Beyond studies of the interaction and conformational motions of *Bs* DHFR with other antifolates, the C73A/S131C$_{MDCC}$ DHFR construct provides a valuable new tool for studying the native state conformational ensemble and the motions of *Bs* DHFR during catalysis; again, giving access to a wide temperature range for studies. The results of the study here suggests the possibility the many enzymes may have multiple conformers that bind at different rates, and the likely importance for the use of extrinsic fluorophores to access information about these conformations and their binding rates [33]. Moreover, the use of extrinsic fluorophores may give new insights into enzyme systems that are not amenable to NMR studies. *Bs* DHFR is stable at a temperature range of 10 - 45°C and the rates (k_1, k_2, k_4) (table 1) are linear with temperature. The Arrhenius and Eyring equations were used to determine thermodynamic parameters; E_a, $\Delta H^{\neq}$, $\Delta S^{\neq}$ and $\Delta G^{\neq}_{298K}$ (Table 2).

References

[1] I. Kompis, K. Islam, R. Then, DNA and RNA synthesis: antifolates., Chemcal Reviews 105 (2005) 593-620.

[2] F.M. Huennekens, The methotrexate story: A paradigm for development of cancer chemotherapeutic agents, Advances in Enzyme Regulation 34 (1994) 397-419.

[3] R.V. Mauldin, M.J. Carroll, A.L. Lee, Dynamic Dysfunction in Dihydrofolate Reductase Results from Antifolate Drug Binding: Modulation of Dynamics within a Structural State, Structure 17 (2009) 386-394.

[4] P. Csermely, R. Palotai, R. Nussinov, Induced fit, conformational selection and independent dynamic segments: an extended view of binding events., Nature Precedings (2010).

[5] G. Hammes, Y.-C. Chang, T. Oas, Conformational selection or induced fit: A flux description of reaction mechanism, Procedings of National Academy of Sciences of the United States of America 106 (2009) 13737-13741.

[6] D.-A. Silva, G. Bowman, A. Sosa-Peinado, X. Huang, A Role for Both Conformational Selection and Induced Fit in Ligand Binding by the LAO Protein. , Public Library of Science Computational Biology 7 (2011) e1002054

[7] K. Johnson, Role of Induced Fit in Enzyme Specificity: A Molecular Forward/Reverse Switch, Journal of Biological Chemistry 283 (2008) 26297-26301.

[8] S.J. Teague, IMPLICATIONS OF PROTEIN FLEXIBILITY FOR DRUG DISCOVERY, Nature Reviews 2 (2003) 527-541.

[9] G. Bhabha, J. Lee, D.C. Ekiert, J. Gam, I.A. Wilson, H.J. Dyson, S.J. Benkovic, P.E. Wright, A Dynamic Knockout Reveals That Conformational Fluctuations Influence the Chemical Step of Enzyme Catalysis, Science 332 (2011) 234-238.

[10] S.P. Sasso, R.M. Gilli, J.C. Sari, O.S. Rimet, C.M. Briand, Thermodynamic study of dihydrofolate reductase inhibitor selectivity, Blochimica et Biophysica Acta 1207 (1994) 74-79.

[11] M. Sawaya, J. Kraut, Loop and Subdomain Movements in the Mechanism of *Escherichia coli* Dihydrofolate Reductase: Crystallographic Evidence, Biochemistry 36 (1997) 586-603.

[12] S. J.R., H.J. Dyson, P.E. Wright, Structure, dynamics, and catalytic function of dihydrofolate reductase., Annual Review of Biochemistry 33 (2004) 119-140.

[13] S.H. Schiffer, S.J. Benkovic, Relating Protein Motion to Catalysis, Annual Review of Biochemistry 75 (2006) 519-541.

[14] H. Pan, J.C. Lee, V.J. Hilser, Binding sites in *Escherichia coli* dihydrofolate reductase communicate by modulating the conformational ensemble, Procedings of National Academy of Sciences of the United States of America 97 (2000) 12020-12025.

[15] N.M. Goodey, S.J. Benkovic, Allosteric regulation and catalysis emerge via a common route, Nature Chemical Biology 4 (2008) 474-482.

[16] C.J. Falzone, P.E. Wright, S.J. Benkovic, Evidence for Two Interconverting Protein Isomers in the Methotrexate Complex of Dihydrofolate Reductase from Escherichia coli, Biochemistry 30 (1991) 2184-2191.

[17] L. Li, C.J. Falzone, P.E. Wright, S.J. Benkovic, Functional Role of a Mobile Loop of *Escherichia coli* Dihydrofolate Reductase in Transition-State Stabilization, Biochemistry 31 (1992) 7826-7833.

[18] C.J. Falzone, P.E. Wright, S.J. Benkovic, Dynamics of a Flexible Loop in Dihydrofolate Reductase from *Escherichia coli* and Its Implication for Catalysis, Biochemistry 33 (1993) 439-442.

[19] J. Adams, K. Johnson, R. Matthews, S.J. Benkovic, Effects of distal point-site mutations on the binding and catalysis of dihydrofolate reductase from Escherichia coli, Biochemistry 28 (1989) 6611-6618.

[20] J.R. Appleman, E.E. Howell, J. Kraut, R.L. Blakley, Role of aspartate 27 of dihydrofolate reductase from Escherichia coli in interconversion of active and inactive enzyme conformers and binding of NADPH, Journal of Biological Chemistry 265 (1990) 5579-5584.

[21] D.D. Boehr, D. McElheny, J.D. H., P.E. Wright, The Dynamic Energy Landscape of Dihydrofolate Reductase Catalysis, Science 313 (2006) 1638-1642.

[22] R. Rajagopalan, Z. Zhang, L. McCourt, M. Dwyer, S. Benkovic, G. Hammes, Interaction of dihydrofolate reductase with methotrexate: Ensemble and single molecule kinetics, Procedings of National Academy of Sciences of the United States of America 99 (2002) 13481-13486.

[23] H.S. Kim, S.M. Damo, S.-Y. Lee, D. Wemmer, J.P. Klinman, Structure and Hydride Transfer Mechanism of a Moderate Thermophilic Dihydrofolate Reductase from *Bacillus stearothermophilus* and Comparison to Its Mesophilic and Hyperthermophilic Homologues, Biochemistry 44 (2005) 11428-11439.

[24] Z.-X. Liang, I. Tsigos, V. Bouriotis, J.P. Klinman, Impact of Protein Flexibility on Hydride-Transfer Parameters in Thermophilic and Psychrophilic Alcohol Dehydrogenases, Journal of American Chemical Society 126 (2004) 9500-9501.

[25] Z.-X. Liang, I. Tsigos, T. Lee, V. Bouriotis, K.A. Resing, N.G. Ahn, J.P. Klinman, Evidence for Increased Local Flexibility in Psychrophilic Alcohol Dehydrogenase Relative to Its Thermophilic Homologue†, Biochemistry 43 (2004) 14676-14683.

[26] S.R. Stone, J.F. Morrison, Kinetic mechanism of the reaction catalyzed by dihydrofolate reductase from Escherichia coli, Biochemistry 21 (1982) 3757-3765.

[27] M. J.F., Kinetics of the reversible inhibition of enzyme-catalysed reactions by tight-binding inhibitors, Biochimica et Biophysica Acta 185 (1969) 269-286.

[28] P. Kuzmic, Program DYNAFIT for the Analysis of Enzyme Kinetic Data: Application to HIV Proteinase, Analytical Biochemistry 237 (1996) 260-273.

[29] L.J. Keith, The Development of the Arrhenius Equation, J Chem. Ed. 61 (1984) 494-498.

[30] H. Eyring, M. Polanyi, Some applications of the transition state method to calculation of reaction velocities, especially in solution, Trans. Faraday Soc. 31 (1935) 875-894.

[31] C.E. Cameron, S.J. Benkovic, Evidence for a Functional Role of the Dynamics of Glycine-121 of *Escherichia coli* Dihydrofolate Reductase Obtained from Kinetic Analysis of a Site-Directed Mutant, Biochemistry 36 (1997) 15792-15800.

[32] O. Oyeyemi, K.M. Sours, T. Lee, K.A. Resing, N.G. Ahn, J.P. Klinman, Temperature dependence of protein motions in a thermophilic dihydrofolate reductase and its relationship to catalytic efficiency, Procedings of National Academy of Sciences of the United States of America 107 (2010) 10074-10079.

[33] N.M. Goodey, M.T. Alapa, D.F. Hagmann, A.K. Mauro, K.S. Kwon, S.M. Hall, Development of a fluorescently labeled thermostable DHFR for studying conformational changes associated with inhibitor binding, Biochim. Biophys. Res. Comm. 413 (2011) 442-447.